Available online at www.sciencedirect.com
SCIENCE DIRECT
Polymer 46 (2005) 7632–7643
polymer
www.elsevier.com/locate/polymer

Toughening of poly(butylene terephthalate) with epoxy-functionalized acrylonitrile–butadiene–styrene

S.L. Sun[a], X.Y. Xu[b], H.D. Yang[b], H.X. Zhang[a,b,*]

[a]*Graduate School, Changchun Institute of Applied Chemistry, Chinese Academy of Sciences, Changchun 130022, China*
[b]*Institute of Chemical Engineering, Changchun University of Technology, Changchun 130012, China*

Received 21 October 2004; received in revised form 9 May 2005; accepted 10 June 2005
Available online 6 July 2005

Abstract

Glycidyl methacrylate (GMA) functionalized acrylonitrile–butadiene–styrene (ABS) copolymers have been prepared via an emulsion polymerization process. These functionalized ABS copolymers (ABS-*g*-GMA) were blended with poly(butylene terephthalate) (PBT). DMA result showed PBT was partially miscible with ABS and ABS-*g*-GMA, and DSC test further identified the introduction of GMA improved miscibility between PBT and ABS. Scanning electron microscopy (SEM) displayed a very good dispersion of ABS-*g*-GMA particles in the PBT matrix compared with the PBT/ABS blend when the content of GMA in PBT/ABS-*g*-GMA blends was relatively low (<8 wt% in ABS-*g*-GMA). The improvement of the disperse phase morphology was due to interfacial reactions between PBT chains end and epoxy groups of GMA, resulting in the formation of PBT-*co*-ABS copolymer. However, a coarse, non-spherical phase morphology was obtained when the disperse phase contained a high GMA content (≥ 8 wt%) because of cross-linking reaction between the functional groups of PBT and GMA. Rheological measurements further identified the reactions between PBT and GMA. Mechanical tests showed the presence of only a small amount of GMA (1 wt%) within the disperse phase was sufficient to induce a pronounced improvement of the impact and tensile properties of PBT blends. SEM results showed shear yielding of PBT matrix and cavitation of rubber particles were the major toughening mechanisms.

Keywords: Poly(butylene terephthalate); Toughening; Epoxy-functionalized ABS

1. Introduction

The enhancement of fracture toughness by incorporation of a rubbery phase in engineering thermoplastic such as polyesters and polyamides has received considerable attention in recent years [1–4]. However, simple blends of these polymers usually cannot obtain satisfactory properties and their phase morphology strongly depends on their processing history. The primary cause of such behavior is the unfavorable interaction between molecular segments of the components, which is responsible for their immiscibility or poor interfacial adhesion. An unfavorable interaction leads to (a) a large interfacial tension in the melt, which makes it difficult to disperse the components finely enough during mixing and drives phase rearrangements during low stress, and (b) poor interfacial adhesion between the two phases, which causes mechanical failure via these weak defects [5].

In order to improve the miscibility of polymer blends and increase interfacial adhesion between matrix and disperse phase, the method of reactive compatibilization is very often used to obtain blends with desirable properties [6–9]. This method is based on the formation of a block or grafted copolymer A–B at the interface between the blend phases during melt mixing. The A–B copolymers can increase interfacial strengths and reduce the droplet coalescence rates through steric repulsion [10–12]. Since most polymer blends do not have the appropriate functional groups, functionalization of the components is very often required [13–15]. In some cases, it is possible to add a third polymer into the blend, which is miscible with one of the blend components and reactive with the other blend component [16–18].

Fortunately, the inherent chemical functionality of

* Corresponding author. Address: Graduate School, Changchun Institute of Applied Chemistry, Chinese Academy of Sciences, Changchun 130022, China. Tel.: +86 431 5826774.
E-mail addresses: ssl@mail.ccut.edu.cn (S.L. Sun), zhanghx@mail.ccut.edu.cn (H.X. Zhang).

0032-3861/$ - see front matter © 2005 Published by Elsevier Ltd.
doi:10.1016/j.polymer.2005.06.011

poly(butylene terephthalate) (PBT) makes it an attractive candidate for modification. Numerous articles describe the approaches that improve the toughness of this material by reacting a polymer containing an appropriate chemical functionality with the carboxyl or hydroxyl end groups of the PBT during melt processing. Functionalized elastomer such as poly(ethylene-*co*-glycidyl methacrylate) (EGMA) has been used for toughening PBT [19]. The epoxy group of GMA can react in situ with the carboxyl and hydroxyl end groups of PBT during melt blending to produce PBT-*g*-EGMA copolymer that can compatibilize the blend. Other rubbers containing GMA, such as EPDM-*g*-GMA [20] and poly(isoprene-*co*-GMA) [21] have been used to toughen PBT by the same mechanism. Maleic anhydride containing elastomers such as EPR-*g*-MA [22], POE-*g*-MA [23,24] and EVA-*g*-MA [25] have also been used to toughen PBT. However, the epoxy functional group appears to be more effective in PBT blend modification than anhydride functional group.

Core-shell impact modifier such as acrylonitrile–butadiene–styrene (ABS) is another important tougher of PBT [26]. The impact properties of PBT can be improved by simple melt blending with appropriate ABS. However, these toughened materials can only be produced within the limited processing range and have unstable phase morphology; the ABS domains can coalesce during certain low shear conditions in the melt resulting in a reduction in mechanical properties. Recently, Lee and co-workers used styrene–acrylonitrile–glycidyl methacrylate (SAG) as a compatibilizer for PBT/ABS blends [27]; Hale and co-workers prepared methyl methacrylate–glycidyl methacrylate–ethyl acrylate (MGE) terpolymer to compatibilize PBT/ABS blends, which makes PBT/ABS blends have more stable morphology [28–32].

In this paper, reactive monomer of GMA was induced to the shell of ABS impact modifier via emulsion polymerization method and the epoxy-functionalized ABS was used to toughen PBT. DMA and DSC were used to study the miscibility of PBT/ABS and PBT/ABS-*g*-GMA blends. The effect of GMA content in ABS-*g*-GMA copolymer on the morphological, rheological, and mechanical properties of PBT blends was studied. SEM was used to observe the fracture morphology and the structure inside the deformed zone of the toughened PBT, and the toughening mechanisms were then proposed.

2. Experimental

2.1. Materials

The poly(butylene terephthalate) (PBT) was purchased from Engineering Plastics Plant of YIHUA Group Corp and its structure is as follows:

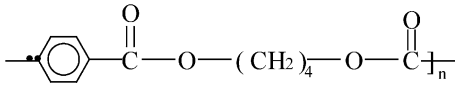

The hydroxyl and carboxyl end-group concentrations are 44 and 20 μequiv./g, respectively. The ABS and ABS-*g*-GMA materials were synthesized by emulsion polymerization method in our lab. The ABS is the typical core-shell architecture polymer as describes in Fig. 1, wherein a soft core, made up of the cross-linked poly(butadiene) (PB), is grafted by a 'shell' of acrylonitrile–styrene (SAN) copolymer. The central nucleus of PB particle provides the soft phase that induces toughening. The shell SAN copolymer allows isolation of the particles from the emulsion by providing a hard coating that keeps the rubbery cores from adhering to one another during the drying process. Table 1 describes the information about ABS and ABS-*g*-GMA materials used in this study. The particle sizes of these materials were determined with a Brookhaven particle size analyzer. The torque measurements of ABS and ABS-*g*-GMA were performed on a Thermo Hakke mixer. The rotating speed was set at 50 rpm and the temperature was set at 230 °C. The torque values list in Table 1 were taken after 10 min in the mixer.

2.2. Preparation of ABS-g-GMA

Functionalization of ABS with GMA was achieved by emulsion polymerization method. In the preparation process a polybutadiene (PB) polymer has to be synthesized first and then AN, St and GMA were polymerized on PB particles. PB latex used in this study was supplied by JILIN Chemical Industry Group synthetic resin factory. The recipe for the preparation of ABS-*g*-GMA is given in Table 2. An oil-soluble initiator, cumene hydro-peroxide (CHP), was used in combination with a redox system. The redox initiator system, CHP, sodium pyrophosphate (SPP), dextrose (DX) and iron (II) sulfate (FeSO4) was used without further purification. The emulsion polymerization was performed in a 2 l glass reactor under nitrogen at 63 °C, and the reaction took place in an alkaline condition at PH10. First, the water, PB, initiator and KOH were added to the glass reactor and stirred 5 min under nitrogen, then the mixture of St/AN (75/25) was added in a continuous feeding way to the glass reactor. After the reaction of St/AN, GMA was added to the

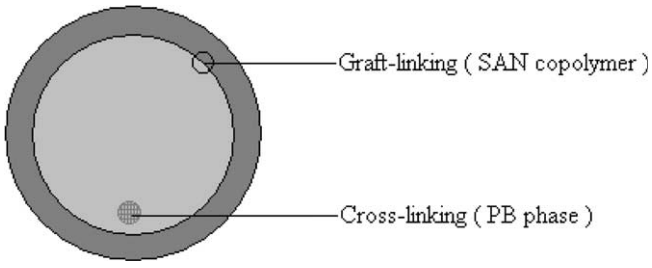

Fig. 1. Diagram of the typical acrylonitrile–butadiene–styrene (ABS) core-shell modifier particle.

Table 1
Properties of ABS and ABS-*g*-GMA used in this study

Designation used here	Rubber content (wt%)	Ratio of AN/St (wt/wt)	GMA content (wt%)	ABS particle size (μm)	Torque (Nm)
ABS	60	25/75	0	0.37	26.2
ABS-*g*-GMA1	60	25/75	1	0.40	26.5
ABS-*g*-GMA3	60	25/75	3	0.41	26.6
ABS-*g*-GMA5	60	25/75	5	0.43	26.2
ABS-*g*-GMA8	60	25/75	8	0.42	26.4

reactor in the same way. The polymers were isolated from the emulsion by coagulation and dried in a vacuum oven at 60 °C for 24 h before being used.

2.3. Reactive blending and molding procedures

The blending was carried out in a twin-screw extruder. Constitutes of PBT/ABS and PBT/ABS-*g*-GMA were 70/30 (wt/wt). The temperature along the extruder were 215, 220, 230, 230, 230, 230,230 °C and the rotation speed of the screw was 60 rpm. The strap of blends were cooled in a water bath and then pelletised.

PBT/ABS and PBT/ABS-*g*-GMA blends were dried in a vacuum oven at 80 °C for 24 h then were injection molded to prepare notched Izod impact specimens and tensile specimens.

2.4. DMA and DSC analysis

The extruded polymer blends were compression molded in order to obtain bars that are suitable for DMA measurements. The polymer blends were melted at 240 °C for 5 min, then a slight pressure was applied. The melted samples were cooled under pressure until solid bars were obtained. These bars were sized $30\times10\times1$ mm^3. The apparatus used is the Netzsch DMA242 (Germany). The scans were carried out in single cantilever mode. The dynamic mechanical measurements were performed over a temperature range from −120 to 150 °C at a constant heating rate of 3 °C/min, and at a frequency of 10 Hz.

Perkin–Elmer DSC-7 was used to study the melting behavior of PBT/ABS and PBT/ABS-*g*-GMA blends. The samples were taken from the injection molded specimens and had a normal weight of about 6 mg. The samples were heated from 0 up to 260 °C at 10 °C/min under a nitrogen atmosphere.

Table 2
The recipe of glycidyl methacrylate-functionalized ABS (in g)

Ingredients	ABS-*g*-GMA
Water	1000
St	3/4 (240–600*x*)[a]
AN	1/4 (240–600*x*)
GMA	600*x*
PB	360
CHP	1.74
SPP	1.5
DX	2.1
$FeSO_4$	0.03
KOH	0.3

[a] *x* indicate the percent of GMA in ABS-*g*-GMA copolymer ($x=0$, 1, 3, 5, 8 wt%).

2.5. Morphological properties

The disperse morphology of ABS and ABS-*g*-GMA in the blends was characterized by scanning electron microscopy (SEM) (model Japan JSM-5600). The sample surface was cut at low temperature with a glass knife until a smooth surface was obtained. Then the samples was etched and coated with a gold layer for SEM observation.

2.6. Rheological properties

The torque measurements of PBT blends were performed on a Thermo Hakke mixer. The rotating speed was set at 50 rpm and the temperature was set at 240 °C.

2.7. Mechanical properties

Notched Izod impact tests of PBT blends were performed at 23 ± 2 °C according to ASTM D256 on a XJU-22 apparatus. The samples with dimensions $63.5\times12.7\times6.35$ mm^3 were obtained from injection molded specimens. The notch was milled in having a depth of 2.54 mm, an angle of 45° and a notch radius of 0.25 mm. The uniaxial tensile tests were carried out at 23 ± 2 °C on an Instron AGS-H tensile tester at a cross-head speed of 50 mm/min according to the ASTM D638. For both mechanical tests at least five samples were tested and their results averaged. The samples were dried overnight prior to testing until the measurement were performed.

3. Results and discussion

3.1. DMA and DSC analysis

The miscibility property between PBT/ABS and PBT/ABS-*g*-GMA blends was studied by DMA. As can be seen in Fig. 2, the peak at 56.7 °C is the T_g of PBT amorphous phase, and the pure ABS exhibits a tan δ peak at 114 °C due to the glass transition of the SAN phase in ABS and a peak at −70 °C due to the T_g of the PB phase. Compared with pure PBT and ABS, the T_g of PBT shift to

high temperature and the T_g of SAN phase shift to low temperature for the PBT/ABS and PBT/ABS-*g*-GMA blends. As we know [33], if the blend displays two T_g's, at or near the two components, then it is immiscible. On the other hand, if it shows a single transition or two transitions at temperature intermediate between those of the pure components, then the blend is miscible or partially miscible. So Fig. 2 shows PBT is partially miscible with ABS and ABS-*g*-GMA copolymer.

DSC was used to study the melting behavior of PBT blends and the corresponding results of the first scan are shown in Fig. 3. As can be seen, the melting point of PBT shifts to lower temperature with the increase in GMA content in PBT/ABS-*g*-GMA blends. Therefore, the miscibility of PBT and ABS was further improved according to the T_m depression criterion [34]. The shift of PBT melting peak to lower temperature is believed to originate from the compatibilization and cross-linking reactions as discussed in the following part. These chemical reactions taking place in the PBT/ABS-*g*-GMA blends will inevitably interface with the crystallization process. It is believed that the increased interaction with the compatibilizer and cross-linking structure hinders the process of crystallization and crystal growth. The chemical reactions lead to increased viscosities can cause a decrease in the crystallization rate. Such effect has been reported by Papadopulou for PET/PP blends compatibilized with SEBS-*g*-MA [35], and by Wendy Loyens for PET/EPR blends compatibilized with E-GMA [36].

3.2. Morphological properties

The morphology of the PBT/ABS and PBT/ABS-*g*-GMA blends was investigated by scanning electron microscopy (SEM). In Fig. 4, all the samples were etched with tetrahydrofuran for 5 h at room temperature to remove ABS phase. The holes left on the surface of the PBT matrix reflect the morphology of the dispersed phase. From the micrographs of Fig. 4, three different kinds of morphology can be observed:

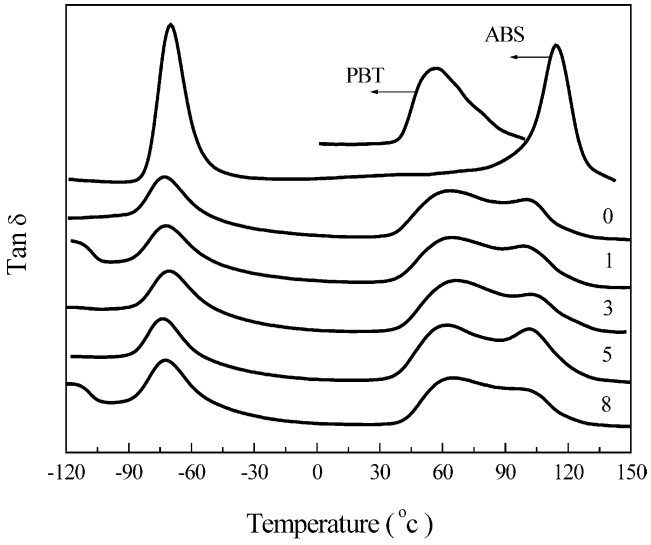

Fig. 2. DMA of PBT, ABS, PBT/ABS and PBT/ABS-*g*-GMA blends with different GMA contents (0-PBT/ABS; 1, 3, 5, 8-PBT/ABS-*g*-GMA1, 3, 5, 8).

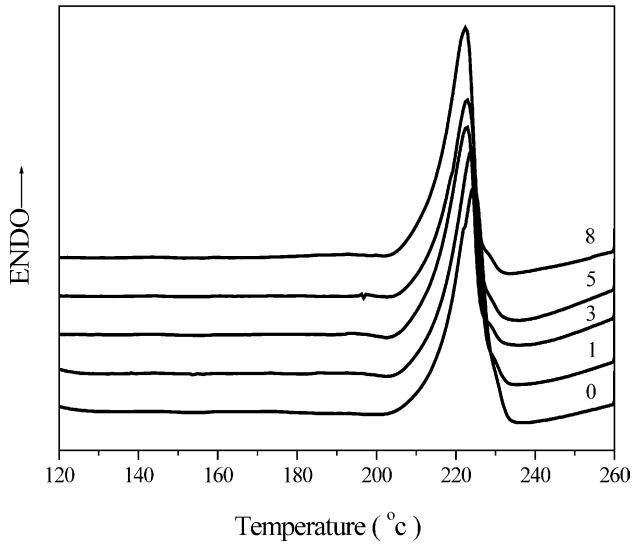

Fig. 3. The melting behavior of PBT/ABS and PBT/ABS-*g*-GMA blends with different GMA contents (0-PBT/ABS; 1, 3, 5, 8-PBT/ABS-*g*-GMA1, 3, 5, 8).

(1) Fig. 4(a) presents the morphology of PBT/ABS blend. When the non-reactive ABS is mixed with PBT, a poor dispersion of ABS particles is obtained. In PBT/ABS blend, some ABS particles cluster together, which will influence the mechanical properties of PBT/ABS blend. The disperse morphology of ABS in PBT matrix proves though PBT is partially miscible with ABS, the interaction between them is not sufficient to suppress the coalescence of ABS particles used in this study. For the simple blend of PBT and ABS, the properties of ABS were very important in order to obtain toughened PBT, and this study will be discussed in a separate paper.

(2) Fig. 4(b)–(d) displays SEM micrographs of the PBT/ABS-*g*-GMA blends with relatively low GMA Content (<8 wt% in ABS-*g*-GMA). It can be seen that in these blends ABS particles disperse in PBT matrix uniformly and the particles have a better spatial distribution. There is no obvious difference in the morphology for the PBT/ABS-*g*-GMA blends with different GMA content.

(3) A different morphology can be observed when the GMA content increases to 8 wt% in the ABS-*g*-GMA8 copolymer. From Fig. 4(e) we can find, in the PBT/ABS-*g*-GMA8 blends, most ABS particles have a good distribution in the PBT matrix, however, there are some large ABS phase domains existing in the blend and the morphology of these domains is very irregular.

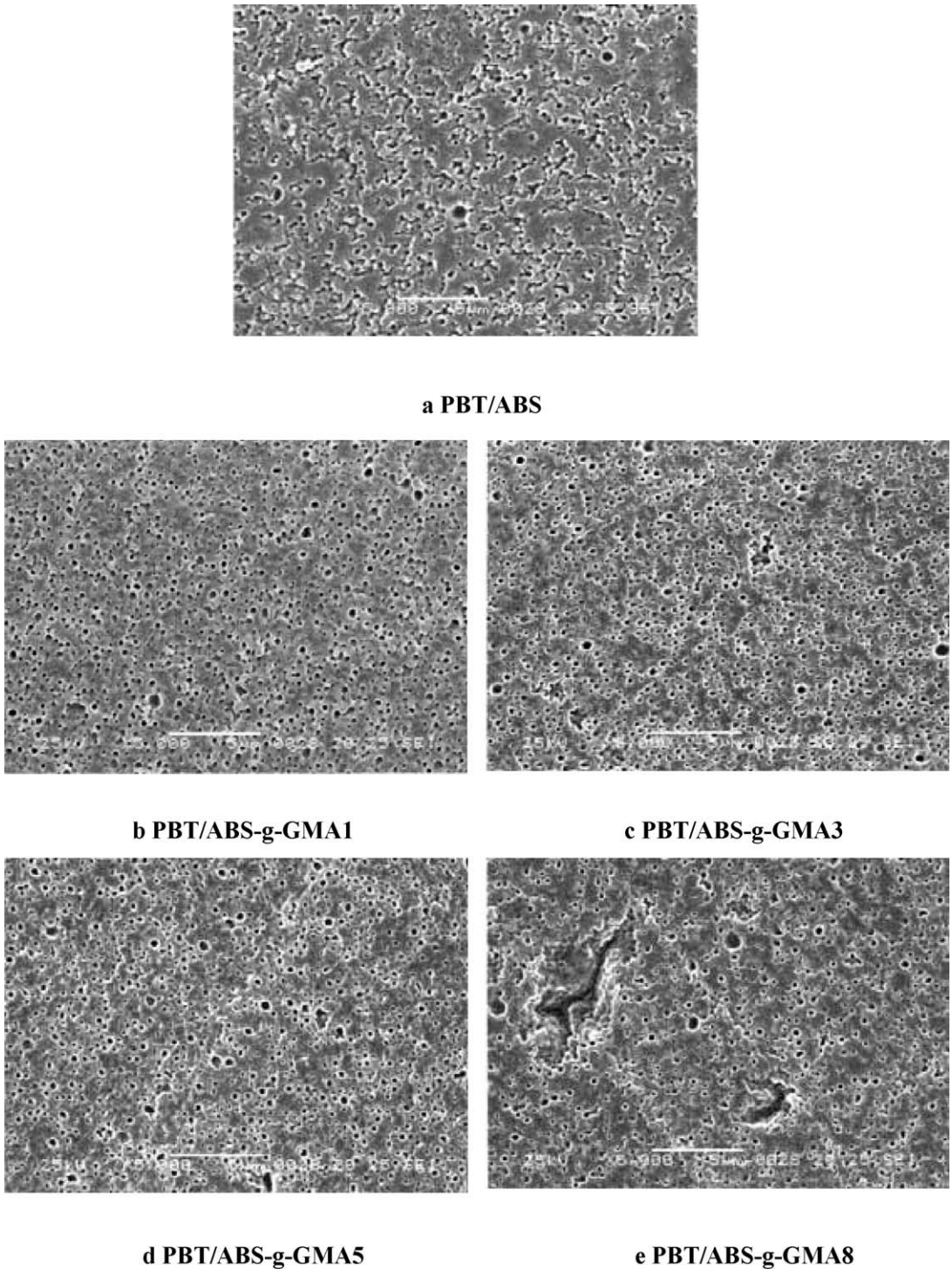

Fig. 4. Morphology of PBT/ABS and PBT/ABS-*g*-GMA blends with different GMA contents (etched with tetrahydrofuran at room temperature).

In order to explain the morphology character of these blends, two types of reactions are identified and shown to take place simultaneously during the reactive blending of PBT and ABS-*g*-GMA (Scheme 1). A few papers have reported on similar reactions involving the GMA functional groups, namely for rubber-modified PBT and PET [37–39]. In a recent publication [40], Martin and his co-workers reported on an analytical study of the compatibilization and cross-linking reactions between GMA and PBT in the PBT/E-GMA blends, and some of their study can be used to explain our experimental results.

Reactions 1 and 2 belong to compatibilization reactions that involve reactions between epoxy groups of ABS-*g*-GMA and carboxyl and hydroxyl end groups of PBT.

Reactions 1 and 2 postulate the formation of PBT-*co*-ABS copolymers at the blend interface. PBT-*co*-ABS copolymer, acting as compatibilizer, can increase interfacial strengths and are believed to promote mixing in two ways. First, disperse phase coalescence rate is reduced through steric repulsion. Second, disperse phase breakup rate is increased through lowered interfacial tension. These factors result in a finer distribution of the disperse phase and response for the better morphological properties of PBT/ABS-*g*-GMA blends.

Reactions 3 and 4 present the cross-linking reactions proposed to occur in PBT/ABS-*g*-GMA blends. The reaction 3 involves the secondary hydroxyl groups present on the copolymers of PBT-*co*-ABS formed at the interface and this reaction takes place in the disperse phase itself. Reaction 4 is based on the bifunctionality of the PBT matrix, as each PBT contains two functional groups that can react with the epoxy groups. In contrast with reaction 3, this cross-linking reaction occurs mainly at the interface. The proposed cross-linking reactions will interfere with the phase morphology formation. The disperse phase will become more viscous and droplet breakup is prevented, resulting in irregular and rough morphology (Fig. 4(e)).

According to several studies [41,42], the rate of interfacial reactions in case of reactive blending should be defined as:

$$\gamma = k_{AB}[A][B] \tag{1}$$

where k_{AB} is the kinetic constant for the reaction between the chemical functions A and B and $[A]$ and $[B]$ are the concentrations of reactive functions A and B, respectively. In this study, the amount of carboxyl and hydroxyl groups in the system was the same for each blend, while the concentration of epoxy groups is increased in ABS-*g*-GMA copolymers. The values of the epoxide/carboxyl and epoxide/hydroxyl concentration ratio are list in Table 3. According to Eq. (1), the formation of PBT-*co*-ABS and the subsequent cross-linking of the rubber phase take place more rapidly in case of PBT/ABS-*g*-GMA blends containing higher GMA contents. However, the difference of reactive ratio between reactions 3 and 4 is obvious. As for the reaction 4, which takes place mainly at the interface, there are some reasons that can lead to its difficult occurrence. First, the concentration of carboxyl, hydroxyl and epoxy groups decrease because of the compatibilization reactions 1 and 2, which will reduce the reactive rate of reaction 4; Second, the viscosity of PBT/ABS-*g*-GMA blends increase due to the compatibilization reactions which is not beneficial to the diffusion of dispersed phase to the interface; Third, the increase in diblock surface density reduces the area available for reactions at the interface, and there is result shows that k_{AB} is exponentially small in diblock surface density [42]. All these factors can prohibit occurrence of reaction 4. Different with reaction 4, reaction 3 takes place in the dispersed phase itself so ABS-*g*-GMA can diffuse in dispersed phase more easily. On the other hand, though the epoxy groups decrease with the occurrence of compatibilization reactions, the hydroxyl groups present on the copolymer of PBT-*co*-ABS increase with the compatibilization reactions. So reaction 3 can still take place in a relatively high reactive rate and this reaction is the main cross-linking reaction in PBT/ABS-*g*-GMA blends.

Fig. 5 shows the disperse morphology of PBT blends in which the PB rubber particles in ABS or ABS-*g*-GMA were

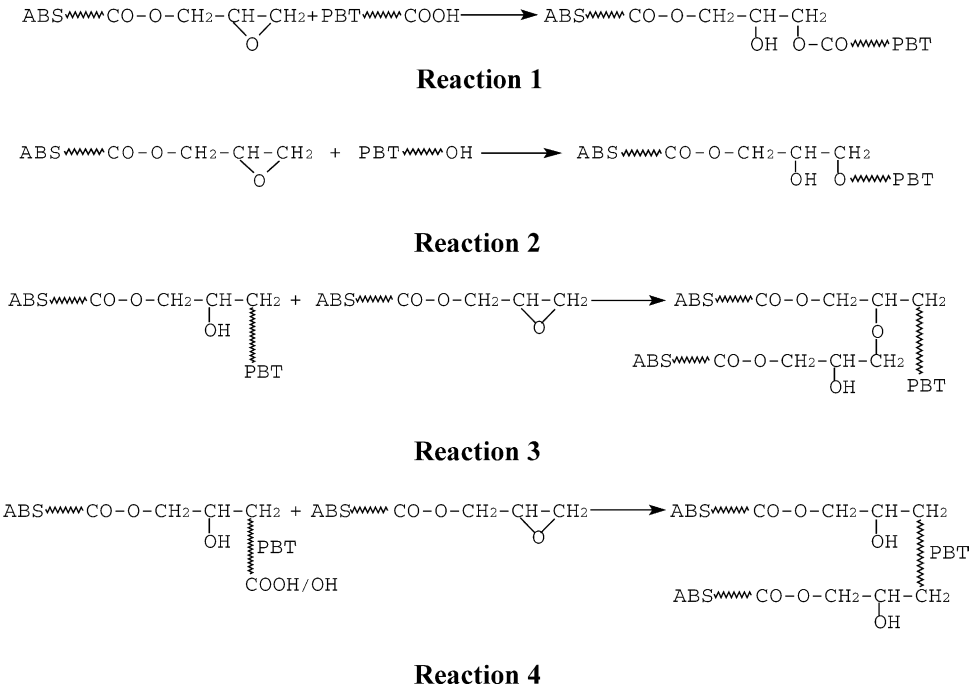

Scheme 1. Reactions in PBT/ABS-*g*-GMA blends.

Table 3
Description of the PBT/ABS-*g*-GMA (70/30, wt/wt) blends and values of the epoxide/COOH and epoxide/OH ratios

Matrix	Dispersed phase	Epoxide/COOH ratio	Epoxide/OH ratio
PBT	ABS	0/20	0/44
PBT	ABS-*g*-GMA1	1.5	0.68
PBT	ABS-*g*-GMA3	4.5	2.04
PBT	ABS-*g*-GMA5	7.5	3.41
PBT	ABS-*g*-GMA8	12	5.45

etched with toluene for 5 h at room temperature. As can be seen from Fig. 5, the PB particles have the similar morphological properties with ABS or ABS-*g*-GMA phase in the blends, which were shown in Fig. 4.

3.3. Rheological properties

Rheological measurements are often used to analyze the occurrence of compatibilization reactions in reactive blending system. Accordingly, simultaneous torque measurements during melt-mixing were performed in order to obtain an idea about the occurring reactions and the viscosity changes. The torque value is related to the viscosity of the blend. A chemical reaction taking place between the reactive blend components will lead to an increase in the blend torque compared to a mixture without any reaction. Fig. 6(a) illustrates the evolution of the torque as a function of the mixing time for PBT/ABS and PBT/ABS-*g*-GMA blends. It can be seen from Fig. 6(a), compared to PBT/ABS-*g*-GMA blends, PBT/ABS has the lowest torque value since there is no chemical reaction between PBT and ABS. For the PBT/ABS-*g*-GMA blends, with the increase in GMA content in PBT/ABS-*g*-GMA blends the torque value of the blends increases too, which further identifies the reaction between the epoxy groups of GMA and the end functional groups of PBT. On the other hand, we find the torque value of all the blends decreases with mixing time due to thermo-decomposition of ABS and PBT because of the high temperature in the mixer (Fig. 6(b)).

Fig. 6(b) illustrates the relation between the actual temperature in the Thermo Hakke mixer and mixing time for PBT/ABS and PBT/ABS-*g*-GMA blends. It can be seen from Fig. 6(b) that the actual temperature in the mixer increases rapidly during a short time interval, and it reaches about 260 °C for the PBT/ABS blend, which is higher than the setting temperature 240 °C due to viscous heating of the polymer even if there is no chemical reaction. For the PBT/ABS-*g*-GMA blends, the temperature in the mixer gets higher. This is partly due to viscous heating of highly viscous PBT-*co*-ABS copolymer or cross-linking polymer and partly due to the exothermic heat of the reactions. The rheological measurements further prove the reactions taking place in the PBT/ABS-*g*-GMA blends.

3.4. Mechanical properties

The typical stress–strain curves for the pure PBT and the PBT/ABS blend are shown in Fig. 7. As it is possible to see, the performance of PBT is strongly modified by ABS addition. The overall effect is a decrease in the values of tensile strength and elongation at break. The pure PBT possesses a tensile strength of about 52 MPa and an elongation at break of 320%. The decrease in tensile strength occurred partly because of the elastomeric nature of PB rubber particles in ABS, on the other hand, the poor interfacial strength between PBT and ABS is an important factor. For the latter reason, the elongation at break decreases seriously.

It is reported that the tensile properties of polymer blends are very sensitive to the state of the interface [43,44], that is, interfacial adhesion. The poor interface behaves as a flaw, and the failure initiates at the interface, which results in low tensile strength and elongation at break. In this study, the interface between PBT and ABS is modified by the introduction of GMA to ABS. According to the reactions 1 and 2 in Scheme 1, the formation of PBT-*co*-ABS copolymer increases the interfacial adhesion strength between PBT and ABS-*g*-GMA. So as shown in Fig. 8(a) and (b), the tensile strength and elongation at break are improved by the introduction of GMA and with the increase in GMA content the tensile properties of PBT/ABS-*g*-GMA blends become much better.

A high improvement of mechanical properties was achieved regarding the toughness (Fig. 8(c)). Notched impact strength of pure PBT is about 50 J/m, while the PBT/ABS blend possesses notched impact strength of about 150 J/m. Although ABS improves the toughness of PBT by a factor of three, which represents a moderate improvement, the blend behaves as a brittle material at impact test. However, the toughness of PBT is improved by the introduction of GMA. Because of the formation of PBT-*co*-ABS copolymer, which acts as compatibilizer, the ABS can disperse in PBT matrix uniformly, so the PBT blends have higher notched impact strength. From Fig. 8(c) we can find the PBT/ABS-*g*-GMA1 blend achieves the highest notched impact strength of 900 J/m, which represents a super-tough behavior. On the other hand, with the increase in GMA content in PBT/ABS-*g*-GMA blends, the notched impact strength of the blends decreases in some degree, and when the content of GMA is 8 wt% the PBT/ABS-*g*-GMA8 blend has the lowest impact strength. The reason of this behavior is the cross-linking reaction between PBT and GMA. The impact property of PBT blends is consistent with their phase morphology.

3.5. Fracture mechanism

In impact tests, the difference between brittle and ductile fracture can be distinguished from the fracture surface of the samples. On a brittle fracture surface stress whitening can

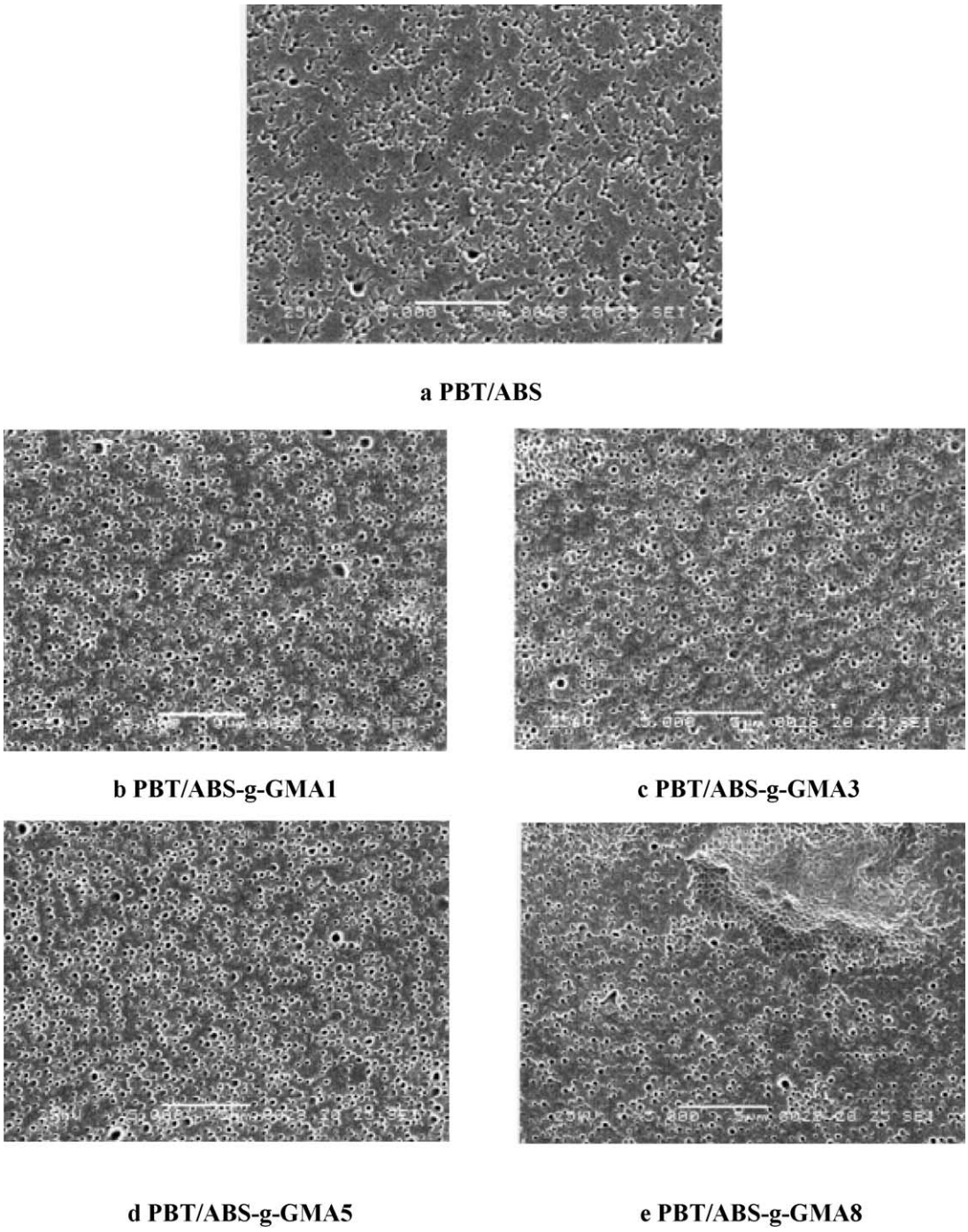

a PBT/ABS

b PBT/ABS-g-GMA1

c PBT/ABS-g-GMA3

d PBT/ABS-g-GMA5

e PBT/ABS-g-GMA8

Fig. 5. Morphology of PBT/ABS and PBT/ABS-*g*-GMA blends with different GMA contents (etched with toluene at room temperature).

only be observed at the origin of the notch tip, but for a tough fracture, all the material around the fracture surface is involved in stress whitening and a yielded zone is formed. The impact strength is related to the size of the yielded zone. A fractured sample with a highly yielded zone usually has higher impact strength.

Fig. 9 provided schematic preparation of samples used for examination of deformation mechanisms in PBT blends by using SEM. The gray areas represent the deformation region. The fracture morphology of PBT/ABS blend is shown in Fig. 10(a). For this blend, the stress whitening can only be seen from the notch tip, and there is no yielded zone on its fracture surface. The PBT phase forms t he matrix and the minor phase of ABS has been segregated into spherical domains. No morphological evidence of good adhesion at the interface between the matrix and the dispersal phase can be seen. The spheres have almost completely smooth surface, and during the fracture process many domains have been pulled away from their previous positions, which remains as empty holes. Fig. 10(b) is the fracture

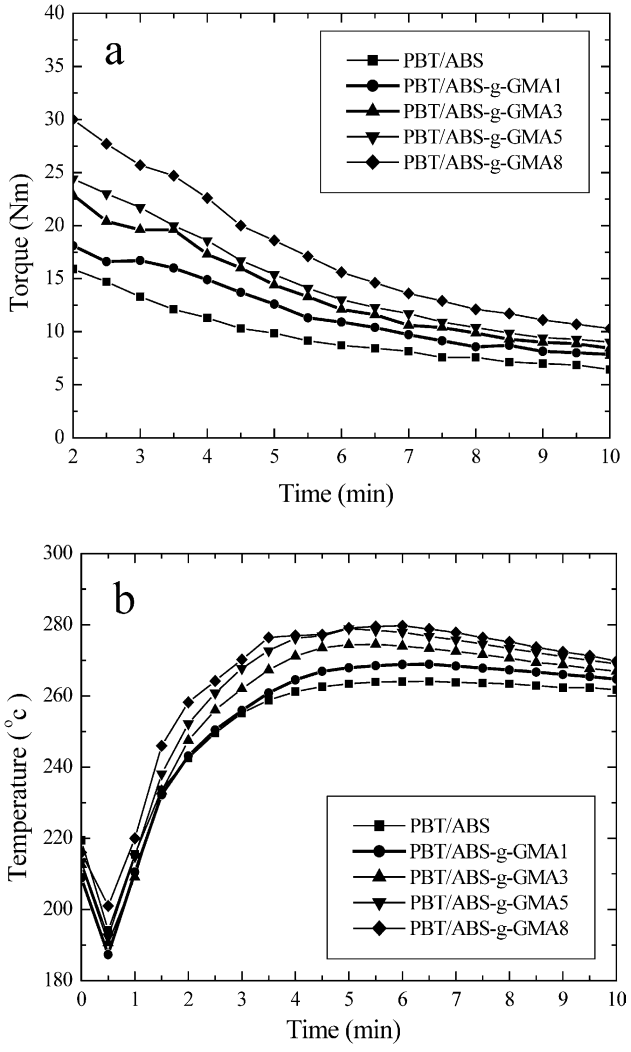

Fig. 6. Evolution of torque (a) and temperature (b) with time in PBT/ABS and PBT/ABS-*g*-GMA blends.

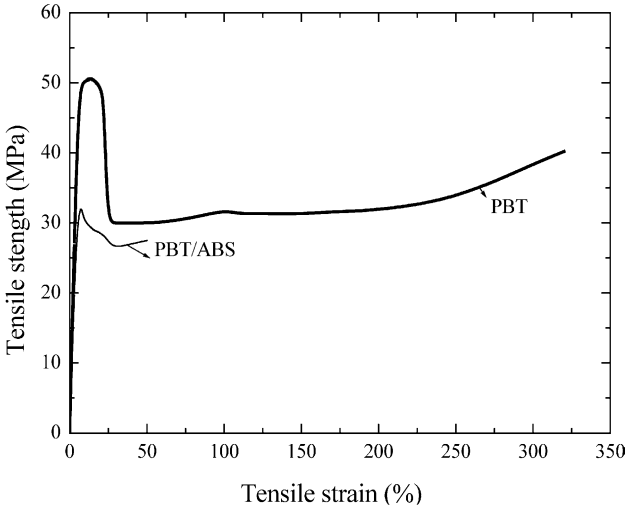

Fig. 7. Tensile behavior of PBT and PBT/ABS blends.

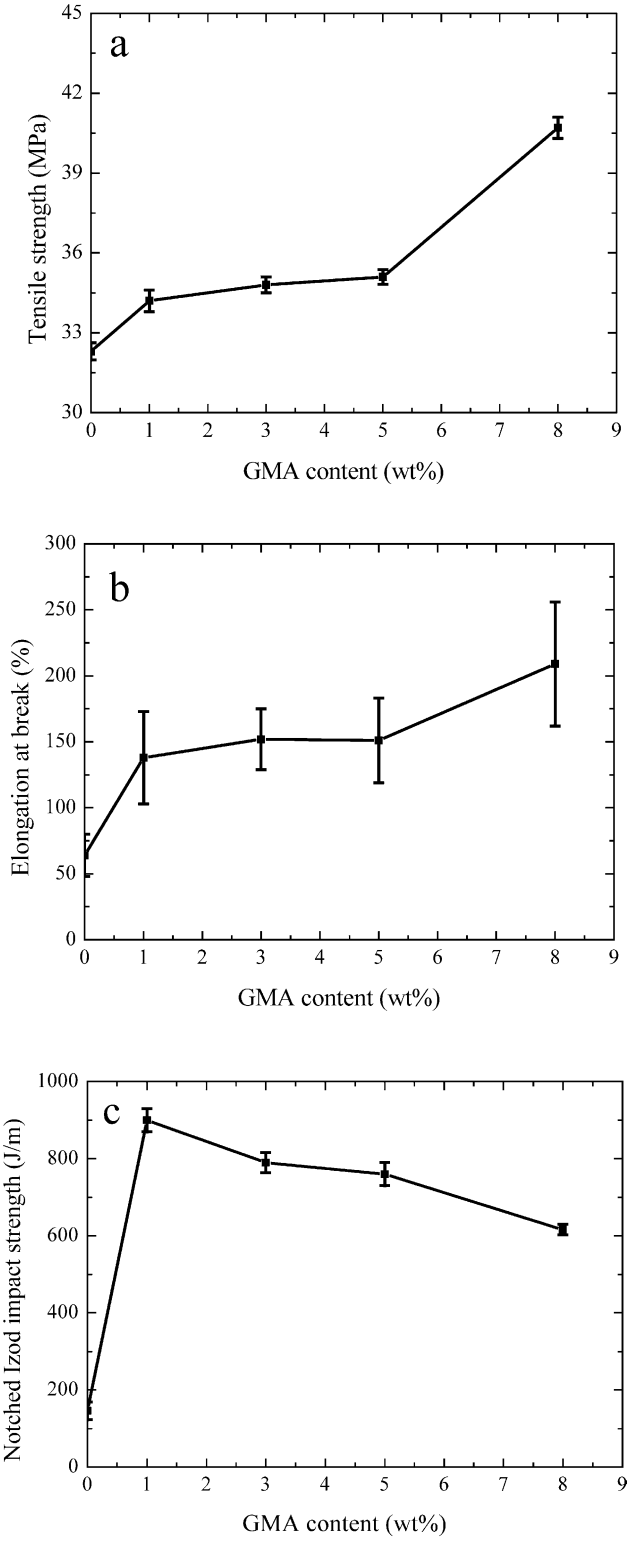

Fig. 8. Mechanical properties of PBT/ABS-*g*-GMA blends with different GMA contents: (a) tensile strength, (b) elongation at break, (c) notched impact strength.

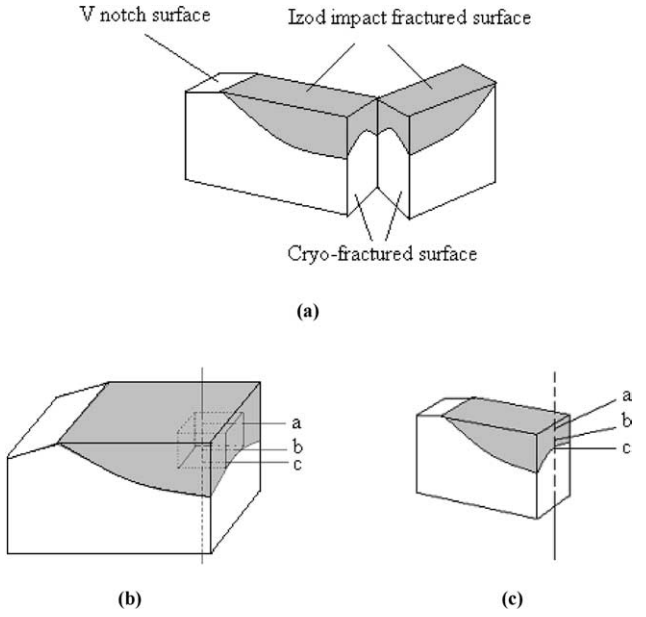

Fig. 9. Schematic presentation of the preparation of samples used for examination of deformation mechanisms in PBT blends by using SEM. The gray areas represent the deformation region.

morphology of PBT/ABS-*g*-GMA1 blend. As expected, the fracture surface of this blend shows the characteristics of ductile fracture. There is extensive plastic deformation, which implies that shear yielding of the PBT matrix has taken place.

In order to correlate the external morphology of the ductile fracture surface to the internal deformation mechanisms of the yielded zone, PBT/ABS-*g*-GMA1 blend was chosen for SEM analysis. A number of scanning electron micrographs were obtained through the stress whitening zone of the sample as defined in Fig. 9, and the sections were taken at different distances from the fracture surface. The surfaces parallel to the notched impact fractured surface (Fig. 9(b)) were cut at low temperature with a glass knife until a smooth surface was obtained. In order to observe the cryo-fractured surface, a saw cut was prepared vertical to the fracture surface only 1 mm away from the stress whitening zone of the broken Izod impact specimen, and the saw cut was sharpened. Then the specimen was immerged in liquid nitrogen for 3 h and torn open immediately, in this way the cryo-fractured surface was prepared for investigation of inner morphology (Fig. 9(c)).

From Fig. 11 we can find, in the surfaces parallel to the notched Izod impact surface, the small holes resulting from voiding of the rubber particles since the samples were not etched and no matrix crazing was observed. The layer containing voids is a so-called cavitation layer. Round voids are observed far from the fracture surface (Fig. 11(c)). The voids increase in size with their position nearer the fracture surface and have a more elongated shape (Fig. 11(b) and

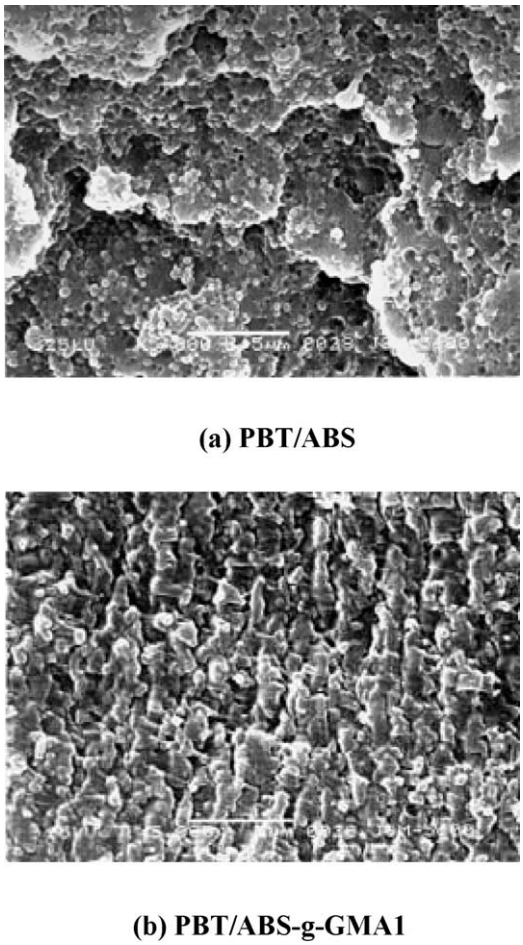

Fig. 10. Morphology of the notched Izod fractured surfaces of PBT/ABS and PBT/ABS-*g*-GMA1 at room temperature as illustrates in Fig. 9(a).

(a)). These elongated voids are formed as a result of the plastic deformation of the surrounding matrix.

Deformed morphology inside the cryo-fractured surface was shown in Fig. 12. Strongly deformed cavities can be seen below the fracture surface with an *L*/*D* ratio of 3–10 and an orientation angle to the fracture surface of $\sim 45°$. These cavitated rubber particles are so highly deformed that they appear to have closed up together, and the matrix around the sheared rubber particles have plastically deformed to a similar degree. The size of the cavities inside the rubber particles diminishes with distance from the fracture surface. At the edge of stress whitening zone (Fig. 12(c)) shear yielding of matrix is not obvious, and only some cavities of rubber particles can be seen.

The micrographs taken in the deformed zone reveal that the stress whitening is a result of cavitation within the rubber particles rather than debonding at the matrix/particle interface. The rubber cavitation is induced by a triaxial stress, and the cavitation extends well beyond the region of shear yielding. It is also apparent that the matrix material has yielded, causing substantial irreversible deformation of the rubber particles. It is clearly shown that shear yielding of the matrix is the major toughening mechanism in these

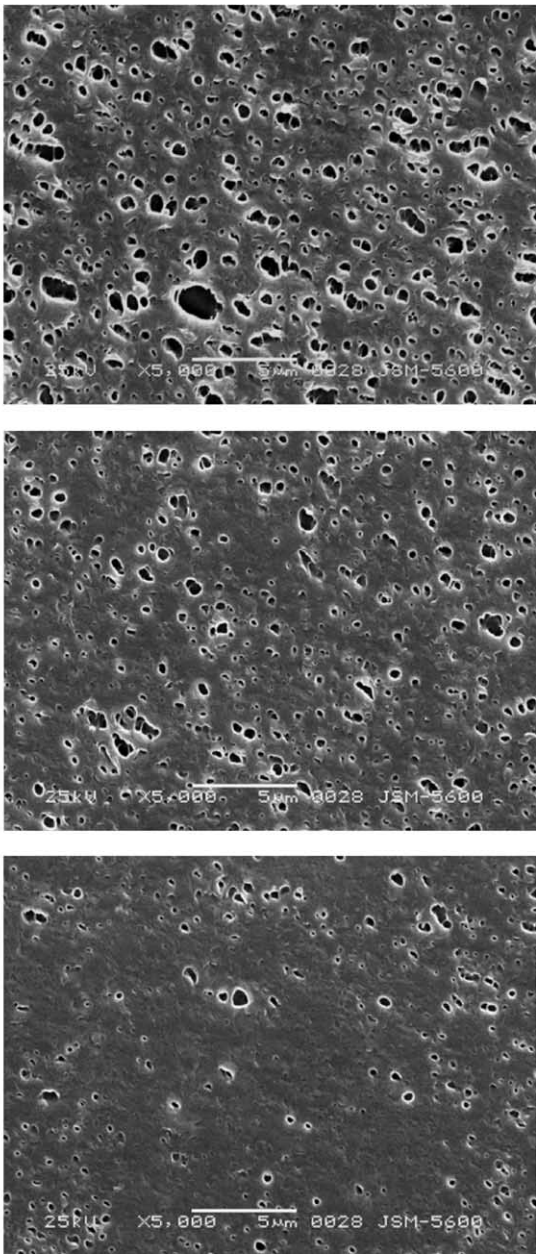

Fig. 11. SEM micrographs in the deformation zone of PBT/ABS-*g*-GMA1 blend. The location of the observed surfaces is illustrated in Fig. 9(b).

impact modified PBT. These results generally agree with the stress–strain transition theory proposed by Yee [45]. The shear yielding is initiated by the stress concentrations associated with rubber particles, consequently, the cavitation of the rubber particles releases the hydrostatic tensile stresses and encourages the shear yielding to proceed.

4. Conclusion

A set of glycidyl methacrylate (GMA) functionalized ABS particles containing various amounts of epoxy groups have been prepared by emulsion polymerization processes.

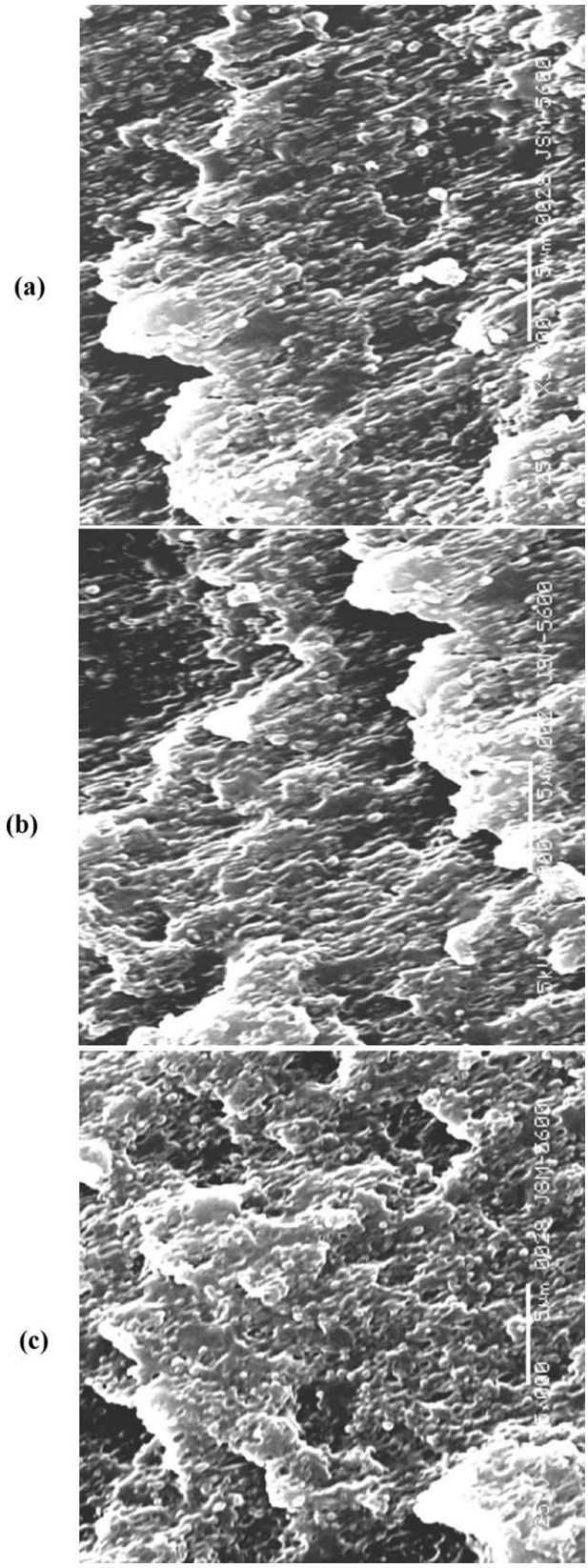

Fig. 12. SEM micrographs of the cryo-fractured surface of PBT/ABS-*g*-GMA1 blend. The location of the observed surface is illustrated in Fig. 9(c).

Experimental results showed epoxy-functionalized ABS particles were very effective to improve the toughness of PBT compared with non-reactive ABS particles.

DMA tests identified PBT was partially miscible with ABS and ABS-*g*-GMA copolymer. DSC results showed the T_m of PBT shift to low temperature with the increase in GMA content, which indicated the introduction of GMA to ABS improved the miscibility of PBT and ABS.

Morphological observation showed when the non-reactive ABS particles were mixed with PBT a poor dispersion of ABS was obtained because of low interfacial adhesion between PBT and ABS. On the other hand, the PBT and the epoxy functionalized ABS blends displayed a fine and complex morphology. In these blends there were two kinds of reactions: (1) compatibilization reactions which involved reactions between ABS-*g*-GMA epoxy groups and both hydroxyl and carboxyl PBT end groups, and (2) cross-linking reaction of ABS-*g*-GMA. When the content of GMA was relatively low (<8 wt%), the cross-linking reaction was not seriously enough to destroy the morphology of the disperse phase in PBT/ABS-*g*-GMA blends (Fig. 4(b)–(d), so PBT/ABS-*g*-GMA blends had a good disperse morphology because of the compatibilization effect. However, when the content of GMA increased to 8 wt%, the cross-linking reaction induced a rough morphology (Fig. 4(e)). Rheological measurements further identified the reactions between PBT and GMA.

Mechanical tests showed the presence of only a small amount of GMA (1 wt%) within the disperse phase was sufficient to induce a pronounced improvement of the impact and tensile properties of PBT blends. On the other hand, the increase in GMA content in the blends induced decrease in notched impact strength of PBT blends due to the cross-linking reaction, which was consistent with the morphological property of PBT/ABS-*g*-GMA blends.

SEM was used to study the toughening mechanisms of PBT blends. The micrographs taken in the deformed zone reveal that the stress whitening is a result of cavitation within the rubber particles rather than debonding at the matrix/particle interface. It is also obvious that the matrix material has yielded. The shear yielding is initiated by the stress concentrations associated with rubber particles, consequently, the cavitation of the rubber particles releases the hydrostatic tensile stresses and encourages the shear yielding to proceed.

Acknowledgements

The project is financially supported by the National Natural Science Foundation of China (grant No. 20074038).

References

[1] Wang XH, Zhang HX, Jiang BZ. Polymer 1997;38:1569.
[2] Brady AJ, Keskkula H, Paul DR. Polymer 1994;35:3665.
[3] Kudva RA, Keskkula H, Paul DR. Polymer 2000;41:225.
[4] Okada O, Keskkula H, Paul DR. Polymer 2001;42:8715.
[5] Paul DR, Bucknall CB. Polymer blends. New York: Wiley; 2000.
[6] Dedecker K, Groeninckx G. Macromolecules 1999;32:2472.
[7] Hyun KJ, Jin KK. Macromolecules 1998;31:9273.
[8] Kelwon C, Kyung HS, Tae OA. J Appl Polym Sci 1998;68:1925.
[9] Yu ZZ, Lei M, Ou YC. Polymer 2002;43:6993.
[10] Creton C, Kramer EJ, Hui CY, Brown HR. Macromolecules 1992;25:3075.
[11] Jin KK, Hwayong L. Polymer 1996;37:305.
[12] Jeon HK, Jin KK. Polymer 1998;39:6227.
[13] Cecere A, Greco R, Ragosta G, Scarinzi G, Taglialatela A. Polymer 1990;31:1239.
[14] Sun YJ, Hu GH, Lambla M, Kotlar HK. Polymer 1996;37:4119.
[15] Hu GH, Sun YJ, Lambla M. Polym Eng Sci 1996;36:676.
[16] Wang XD, Li HQ. J Appl Polym Sci 2000;77:24.
[17] Araujo EM, Hage E, Carvalho AJF. J Appl Polym Sci 2002;87:842.
[18] Dedecker K, Groeninckx G. Polymer 1998;39:4985.
[19] Arostegui A, Nazabal J. J Polym Sci, Part B: Polym Phys 2003;41:2236.
[20] Phadke SV. US Patent 5 008 342; 1991.
[21] Modic MJ. (Shell Oil Co), US Patent 5 300 567; 1994.
[22] Cecer A, Greco R, Ragosta G, Scarinzi G. Polymer 1990;31:1239.
[23] Arostegui A, Gaztelumendi M, Nazabal J. Polymer 2001;42:9565.
[24] Arostegui A, Nazabal J. Polymer 2003;44:239.
[25] Seon-Jun K, Bong-Sub S, Jeong-Lag H, Won-Jei C, Chang-Sik H. Polymer 2001;42:4073.
[26] Hage E, Hale W, Keskkula H, Paul DR. Polymer 1997;38:3237.
[27] Pei-Ching L, Wen-Faa K, Feng-Chih C. Polymer 1994;35:5641.
[28] Hale W, Keskkula H, Paul DR. Polymer 1999;40:365.
[29] Hale W, Keskkula H, Paul DR. Polymer 1999;40:3665.
[30] Hale W, Keskkula H, Paul DR. Polymer 1999;40:4237.
[31] Hale W, Keskkula H, Paul DR. Polymer 1999;40:3621.
[32] Hale W, Keskkula H, Paul DR. Polymer 1999;40:3353.
[33] Sudhin D, David JL. Polymer compatibilizers. Munich: Hanser Publishers; 1996.
[34] Hage E, Ferreira LAS, Manrich S, Pessan LA. J Appl Polym Sci 1999;71:423.
[35] Papadopoulou CP, Kalfoglou NK. Polymer 2000;(41):2543.
[36] Loyens W, Groeninckx G. Polymer 2002;43:5679.
[37] Loyens W, Groeninckx G. Macromol Chem Phys 2002;203:1702.
[38] Yu ZZ, Yan C, Dasari A, Dai SC, Mai YW, Yang MS. Macromol Mater Eng 2004;289:763.
[39] Loyens W, Groeninckx G. Polymer 2003;44:123.
[40] Martin P, Devaux J, Legras R, van Gurp M, van Duin M. Polymer 2001;42:2463.
[41] Martin P, Gallez C, Devaux J, Legras R, Leemans L, van Gurp M, et al. Polymer 2003;44:5251.
[42] O'Shaughnessy B, Sawhney U. Macromolecules 1996;29:7230.
[43] Legros A, Carreau PJ, Favis BD, Michel A. Polymer 1994;35:758.
[44] Oshinski AJ, Keskkula H, Paul DR. Polymer 1992;33:28.
[45] Yee AF. J Mater Sci 1977;12:759.